Turbulence during H and L-mode plasmas in the scrape-off layer of the ASDEX Upgrade tokamak

G. Y. Antar[†], M. Tsalas, E. Wolfrum, V. Rohde and the ASDEX Upgrade Team

Max-Planck Institut für Plasmaphysik, Boltzmannstr. 7, 85748 Garching, Germany
[†] American University of Beirut, Riad El-Solh, Beirut 1107 2020, Lebanon

Abstract.

We present evidence showing that the statistical properties of turbulence in the scrape-off layer (SOL) are not modified in a high-confinement mode (H-mode) in-between edge-localized modes (ELMs) with respect to a low confinement mode (L-mode). The plasma being in the upper-single null magnetic configuration, the reciprocating probe around the bottom X-point is used characterize in the same discharge the low and the high-field scrape-off layer. In H-mode in-between ELMs, the average value and the standard deviation of the ion saturation current are found very close to values in L-mode. The normalized standard deviation is found to have the same values as in L-mode independently of the probe position. The probability distribution function is found similar in the two regimes reflecting the two transport processes, diffusion and convection, are not modified with respect to each other. The power spectra were found similar as well indicating the same distribution of the turbulence intensity among the scales in L and H-mode. The plasma profiles in the SOL, determined using the lithium beam diagnostic, were found to have the same shape as a function of the radial position also reflecting the non-modification of the transport properties in L and H-mode.

1. Introduction

Even after almost three decades of discovering the high confinement mode (H-mode) on the ASDEX tokamak [1], the role of turbulent transport is still ambiguous. It was postulated that the transition from a low confinement mode (L-mode) to H-mode might be caused by the radial electric shear [2]. However, this has not been firmly confirmed in toroidal fusion devices and remains an open issue. Much of the interest was and is still focused on the fluctuations during edge localized modes (ELMs) [3] which can be interpreted as caused by turbulent fluctuations [4, 5]. The understanding of the behavior of turbulence in-between ELMs is motivated by various fundamental and engineering aspects. The fundamental aspects can be summarized in the nature of H-mode and the reason behind the profiles steepening inside the separatrix. From the engineering point of view, it is important to accurately assess the particle fluxes on the first walls not only during ELMs but also in-between. It can be shown, as for example hereafter, that the plasma flux on the vessel walls for high density discharges during ELMs may not be that different from the ELM-free phase.

Recently, a series of investigations were made mainly in low confinement (L-mode) plasmas to understand the transport across the scrape-off layer (SOL). It was shown that intermittency is caused by convective large-scale structures that are called avaloids [6] or blobs [7]. Moreover, this transport has a universal character caused by similar properties of turbulence on various devices [8]; this was confirmed by additional investigations [9–11]. Convective transport that denotes large-scale structures with large radial velocities was studied on linear devices where it was shown that avaloids can be associated with small poloidal mode numbers [12]. At the same time, models and numerical simulations were developed to simulate convective transport showing good agreement with the experiment [13–15]. Most of the experimental results were done in L-mode plasmas, but the few investigations in H-mode suggested that neither the level of turbulence nor the skewness and flatness factors are modified [5, 16, 17]. Results from the Thomson scattering on ASDEX upgrade have shown the existence of local maxima and minima in the temperature and density in-between ELMs leading to a rather large and systematic

variations in the plasma profiles [18, 19].

This letter compares the statistical properties turbulence in the SOL in L and H-mode. It is found that turbulence in-between ELMs in upper-single null H-mode plasmas is very similar to L-mode where both the diffusive and convective transport processes are unaffected. Moreover, the distribution of the fluctuations among the turbulent scales, reflected in the power spectrum, is not modified. These facts hold for both the high and the low field sides.

2. The Experimental Setup

The experiment is performed on the ASDEX Upgrade tokamak [20] where the main plasma properties for four discharges used hereafter are shown in Fig. 1. The discharges 21284 and 21285 are selected because the average density in the H-mode phase ($6 > t > 3.5$) is low leading to a significant time interval between ELMs simplifying the comparison to L-mode. The shots 20356 and 20357 are used because they have the same plasma parameters (magnetic field -2 Tesla, plasma current 0.8 MA, shape and especially the Greenwald density) except for the 5 MW neutral beam heating in the second whereas 20356 is only ohmically heated. In the four discharges, the plasma is in the upper-single null (USN) magnetic configuration allowing the the X-point Demokritos probe [21], located at the bottom of the tokamak, to perform its reciprocations without having to be in the proximity of the separatrix. The radial position of the lower X-point is about 1.5 m. Four reciprocations are performed two in L and two in H-mode for each discharge. The probe first goes into the low-field SOL, then around the lower X-point into the high-field SOL and back. The probe travel on the low-field side maps a distance between 2 and 3 cm at the mid-plane.

3. The Ion Saturation Current in the SOL of L and H-mode Plasmas

In Fig. 2(a) is shown the ion saturation current I_{sat} as a function of time for two discharges 21284 and 21285 in L and H-mode. The upper limit of the y-axis in H-mode was reduced cutting up the ELMs contribution in order to highlight the plasma behavior in-between ELMs. A zoom on the time in-between ELMs is done in (b) where one can

visually realize that not only the absolute values of I_{sat} in L and H-mode are close but also the level of turbulence and the nature of the fluctuations.

A detailed statistical analysis shows that, while both the absolute value and the level of fluctuations are slightly higher in H than in L-mode in consequence of the higher average density in H-mode, the relative level of fluctuations is the same in both discharges. This is shown Fig. 4(a) where the normalized level of fluctuations is plotted and the result is in agreement with Ref. [16, 17]. Furthermore, Fig. 4(a) shows that the relative level of fluctuations in the two operational regimes is very close not only on the high- but also on low-field sides.

In Fig. 2(c) is plotted the same thing as in (a) but for the discharges 20356 and 20357 where the average density is the same along with the other plasma parameters. As plasma turbulence depends strongly on the average density [22], the main point here is to use discharges with the same average density to compare H (in-between ELMs) to L-mode. Here also, I_{sat} is roughly the same in both discharges and a detailed analysis revealed that the level of fluctuations is the same for all probe positions (high and low-field sides). The zoom in (d) clearly shows that the average and the level of fluctuations are very close in-between ELMs and in L-mode.

Fig. 2 offers yet the most direct comparison of turbulence behavior in L and H-mode simultaneously on the low and the high-field sides.

4. Statistical Properties and the Behavior of Turbulence in L and H-mode

The statistical properties of turbulence in the SOL are investigated using the probability distribution function (PDF) and the power spectra (P_f). The same number of points is selected in L and H-mode and I is calculated by subtracting its average value, determined over a period of 10 ms, from I_{sat} and then normalizing the result by the standard deviation. In Fig. 3(a) is illustrated the PDF of I in L-mode and in-between ELMs in H-mode where the probe is in the low-field SOL. The two curves are very similar and agree well with the PDFs that were published in L-mode plasmas on other fusion devices [8]. Negative fluctuations of I has a parabolic shape which reflects a Gaussian distribution. This is interpreted as the contribution of turbulent diffusion with a rare

presence of coherent structures. The PDF for positive I's, on the other hand, is far from Gaussian possessing an exponential tail. This part is dominated by the contribution of the intermittent bursts that were shown to be caused by large-scale and large radial velocity events in L-mode. The determination of the flatness and skewness factors as a function of the probe position was performed and plotted in Fig. 4(b) and (c). Excellent agreement is found for all the probe positions in H and L modes; a similar result was obtained on DIII-D for the low field side [17]. The fact that the two PDFs agree so well reflects that, the amplitude of the fluctuations, their distribution and their probability of occurrence are very close in the two operational modes.

In Fig. 3(b), we illustrate the power spectra of I in L and H-mode and here again the agreement is excellent. As for L-mode, the power spectra have only one scaling region with an exponent about -1.6. This comparison was performed for all probe positions as it scans the low and the high field sides and the same agreement was obtained indicating that the spectra shape are not modified in the two regimes. Accordingly, the power distribution among the turbulent scales is unchanged in H (in-between ELMs) when compared to L-mode. In other words, the small scales are affected at the same level as large ones, if any, in the L to H transition and this hold for the low as well as the high field sides.

5. Average Profiles Behavior

To address the issue of the SOL properties at the mid-plane we use the lithium beam diagnostic to obtain the average radial profile of the density. If the above results were accurate, the profiles shape must be unaffected in L and H-mode. For the shots 20356 and 20357 plotted in Fig. 5(a) the profiles are almost identical. We recall that their average core density is the same. For 21284 and 21285 plotted in Fig. 5(b), the profiles are different reflecting the difference in the average density. However, as the two profiles are normalized to the density at the separatrix (Fig. 5(c)), they end up having the same radial profile. Accordingly, this is an independent and additional argument that the processes that underlines radial transport at the edge are unchanged by the L to H transition. We emphasize, that time-averaged profiles are not 'real' plasma profiles as

turbulent fluctuations exist leading to systematic statistical variations as it was shown in Ref. [18] and as one can see in Fig. 5(c) where Thomson scattering profiles of density at the mid-plane is included. Moreover, Fig. 5(c) suggests that the level of fluctuations of the density is unaltered in the L to H transition in agreement with the probe data.

6. Conclusion

It was shown in a rather straightforward fashion that the statistical properties of turbulence are not modified in H-mode when compared to L-mode SOL. The underlying mechanisms of transport, that are turbulent diffusion by eddies and convective transport by avaloids (or blobs), are thus not modified. In other words, they are unchanged in terms of relative intensity and probability of occurrence as it was shown using the probability distribution function. Furthermore, since the power spectra are unchanged in the two regimes, one can rather safely deduce that the distribution of fluctuations among the turbulence scales is not modified. In this case, large scales are not more affected than smaller ones or *vice versa*. In addition, we have shown that neither the level of turbulence in the SOL nor the mid-plane profiles are modified in the shots studied here. Transport modification during the L to H transition, if any, is thus done on equal footage between large and small scales, diffusive and convective transport, on the low and high-field sides. Consequently, this paper shows that suppression or modification of turbulence in the SOL is neither a necessary nor a sufficient condition to achieve H-mode in tokamaks. However, we believe that the above analyses should be applied to other types of H-modes in order to have a more precise idea about the behavior of turbulence in the SOL during H-mode

[1] Wagner F, Becker G, Behringer K, Campbell D, Eberhagen A, Engelhardt W, Fussmann G, Gehre O, Gernhardt J, Gierke G v, Haas G, Huang M, Karger F, Keilhacker M, Klüber O, Kornherr M, Lackner K, Lisitano G, Lister G G, Mayer H M, Meisel D, Müller E R, Murmann H, Niedermeyer H, Poschenrieder W, Rapp H and Röhr H 1982 *Phys. Rev. Lett.* **49**(19) 1408–1412

[2] Biglari H, Diamond P H and Rosenbluth M N 1989 *Phys. Fluids* **1** 109

[3] Kirk A, Eich T, Herrmann A, Mueller H W, Horton L D, Counsell G F, Price M, Rohde V, Bobkov V, Kurzan B, Neuhauser J, Wilson H, the ASDEX Upgrade and Teams M 2005 *Plasma Physics and Controlled Fusion* **47**(7) 995–1013 URL `http://stacks.iop.org/0741-3335/47/995`

[4] Antar G Y, Counsell G and Ahn J W 2005 *Physics of Plasmas* **12**(8) 082503 (pages 11) URL `http://link.aip.org/link/?PHP/12/082503/1`

[5] Rudakov D L, Boedo J A, Moyer R A, Stangeby P C, Watkins J G, Whyte D G, Zeng L, Brooks N H, Doerner R P, Evans T E, Fenstermacher M E, Groth M, Hollmann E M, Krasheninnikov S I, Lasnier C J, Leonard A W, Mahdavi M A, McKee G R, McLean A G, Pigarov A Y, Wampler W R, Wang G, West W P and Wong C P C 2005 *Nuclear Fusion* **45** 1589

[6] Antar G Y, Krasheninnikov S I, Devynck P, Doerner R P, Hollmann E M, Boedo J A, Luckhardt S C and Conn R W 2001 *Phys. Rev. Lett.* **87** 065001

[7] Krasheninnikov S I 2001 *Phys. Lett. A* **283** 368

[8] Antar G, Counsell G, Yu Y, LaBombard B and Devynck P 2003 *Phys. Plasmas* **10** 419

[9] Xu Y H, Jachmich S, Weynants R R and the TEXTOR team 2005 *Plasma Physics and Controlled Fusion* **47**(10) 1841–1855 URL `http://stacks.iop.org/0741-3335/47/1841`

[10] van Milligen B P, Sanchez R, Carreras B A, Lynch V E, LaBombard B, Pedrosa M A, Hidalgo C, Goncalves B, Balbin R and Team W A (W7-AS Team) 2005 *Physics of Plasmas* **12**(5) 052507 (pages 7) URL `http://link.aip.org/link/?PHP/12/052507/1`

[11] Carter T A 2006 *Physics of Plasmas* **13**(1) 010701 (pages 4) URL `http://link.aip.org/link/?PHP/13/010701/1`

[12] Antar G Y, Yu J H and Tynan G 2007 *Physics of Plasmas* **14**(2) 022301 (pages 10) URL `http://link.aip.org/link/?PHP/14/022301/1`

[13] Pigarov A Y, Krasheninnikov S I, Rognlien T D, Schaffer M J and West W P 2002 *Physics of Plasmas* **9**(4) 1287–1299 URL `http://link.aip.org/link/?PHP/9/1287/1`

[14] Krasheninnikov S I, Smolyakov A I and Soboleva T K 2005 *Physics of Plasmas* **12**(7) 072502 (pages 5) URL `http://link.aip.org/link/?PHP/12/072502/1`

[15] Garcia O E, Bian N H, Naulin V, Nielsen A H and Rasmussen J J 2005 *Physics of Plasmas* **12**(9) 090701 (pages 4) URL `http://link.aip.org/link/?PHP/12/090701/1`

[16] Moyer R A, Rhodes T L, Rettig C L, Doyle E J, Burrell K H, Cuthbertson J, Groebner R J, Kim K W, Leonard A W, Maingi R, Porter G D and Watkins J G 1999 *Plasma Physics and Controlled Fusion* **41**(2) 243–249 URL `http://stacks.iop.org/0741-3335/41/243`

[17] Rudakov D L, Boedo J A, Moyer R A, Krasheninnikov S, Leonard A W, Mahdavi M A, McKee G R, Porter G D, Stangeby P C, Watkins J G, West W P, Whyte D G and Antar G 2002 *Plasma Physics and Controlled Fusion* **44**(6) 717–731 URL `http://stacks.iop.org/0741-3335/44/717`

[18] Kurzan B, Murmann H D, Neuhauser J and the ASDEX Upgrade Team 2005 *Physical Review Letters* **95**(14) 145001 (pages 4) URL `http://link.aps.org/abstract/PRL/v95/e145001`

[19] Kurzan B, Murmann H D, Neuhauser J and the ASDEX Upgrade Team 2007 *Plasma Phys. Control. Fusion*

[20] Gruber O, Arslanbekov R, Atanasiu C, Bard A, Becker G, Becker W, Beckmann M, Behler K, Behringer K, Bergmann A, Bilato R, Bolshukin D, Borrass K, Bosch H S, Braams B, Brambilla M, Brandenburg R, Braun F, Brinkschulte H, Brückner R, Brüsehaber B, Büchl K, Buhler A, Bürbaumer H, Carlson A, Ciric M, Conway G, Coster D, Dorn C, Drube R, Dux R, Egorov S, Engelhardt W, Fahrbach H U, Fantz U, Faugel H, Foley M, Franzen P, Fu P, Fuchs J, Gafert J, Gantenbein G, Gehre O, Geier A, Gernhardt J, Gubanka E, Gude A, Günter S, Haas G, Hartmann D, Heinemann B, Herrmann A, Hobirk J, Hofmeister F, Hohenöcker H, Horton L,

Hu L, Jacobi D, Jakobi M, Jenko F, Kallenbach A, Kardaun O, Kaufmann M, Kendl A, Kim J W, Kirov K, Kochergov R, Kollotzek H, Kraus W, Krieger K, Kurzan B, Kyriakakis G, Lackner K, Lang P, Lang R, Laux M, Lengyel L, Leuterer F, Lorenz A, Maier H, Mank K, Manso M E, Maraschek M, Mast K F, McCarthy P, Meisel D, Meister H, Meo F, Merkel R, Mertens V, Meskat J, Monk R, Müller H, Münich M, Murmann H, Neu G, Neu R, Neuhauser J, Noterdaeme J M, Nunes I, Pautasso G, Peeters A, Pereverzev G, Pinches S, Poli E, Pugno R, Raupp G, Ribeiro T, Riedl R, Riondato S, Rohde V, Röhr H, Roth J, Ryter F, Salzmann H, Sandmann W, Sarelma S, Schade S, Schilling H B, Schlögl D, Schmidtmann K, Schneider R, Schneider W, Schramm G, Schweinzer J, Schweizer S, Scott B, Seidel U, Serra F, Sesnic S, Sihler C, Silva A, Sips A, Speth E, Stäbler A, Steuer K H, Stober J, Streibl B, Strumberger E, Suttrop W, Tabasso A, Tanga A, Tardini G, Tichmann C, Treutterer W, Troppmann M, Tsois N, Ullrich W, Ulrich M, Varela P, Vollmer O, Wenzel U, Wesner F, Wolf R, Wolfrum E, Wunderlich R, Xantopoulos N, Yu Q, Zarrabian M, Zasche D, Zehetbauer T, Zehrfeld H P, Zeiler A and Zohm H 2001 *Nuclear Fusion* **41**(10) 1369–1389 URL `http://stacks.iop.org/0029-5515/41/1369`

[21] Tsalas M, Tsois N, Rohde V and Neuhauser J 2005 *Journal of Nuclear Materials* **337-339** 751–755

[22] Antar G 2003 *Phys. Plasmas* **10** 3629

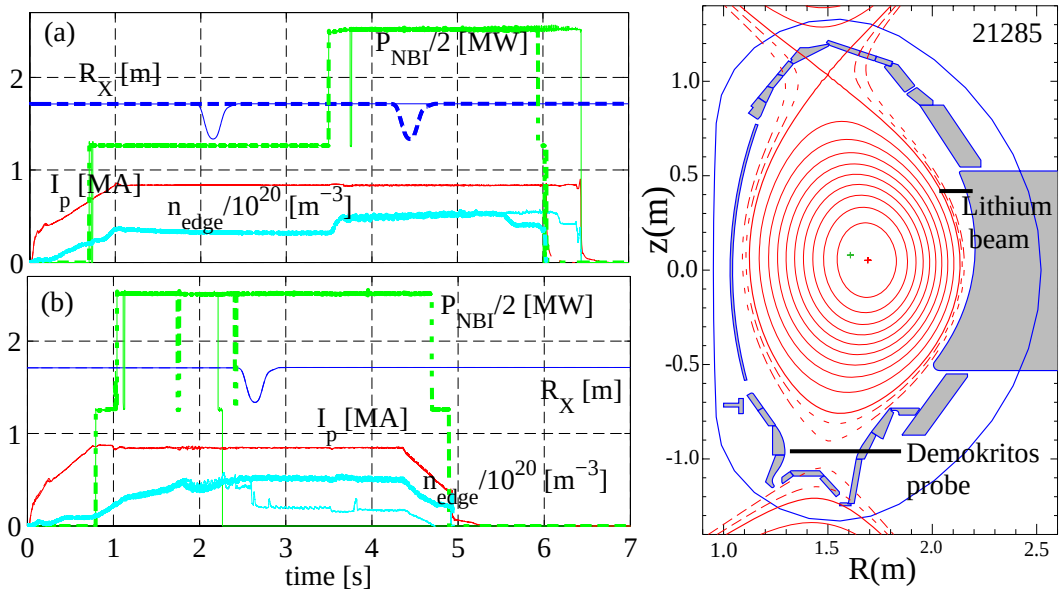

Figure 1. (a) shows the plasma parameters of two discharges 21284 and 21285. The probe position is R_X plunging at 2.2 and 4.5 s. In (b) is illustrated the main parameters of the two discharges 20356 and 20357 where the probe plunges at 2.6 s. Note that the neutral beam heating was shut down 300 ms before the probe plunges in 20357. The right-hand plot shows a magnetic reconstruction graph of shot 21285 where we inserted the positions of the lithium beam and the Demokritos probe.

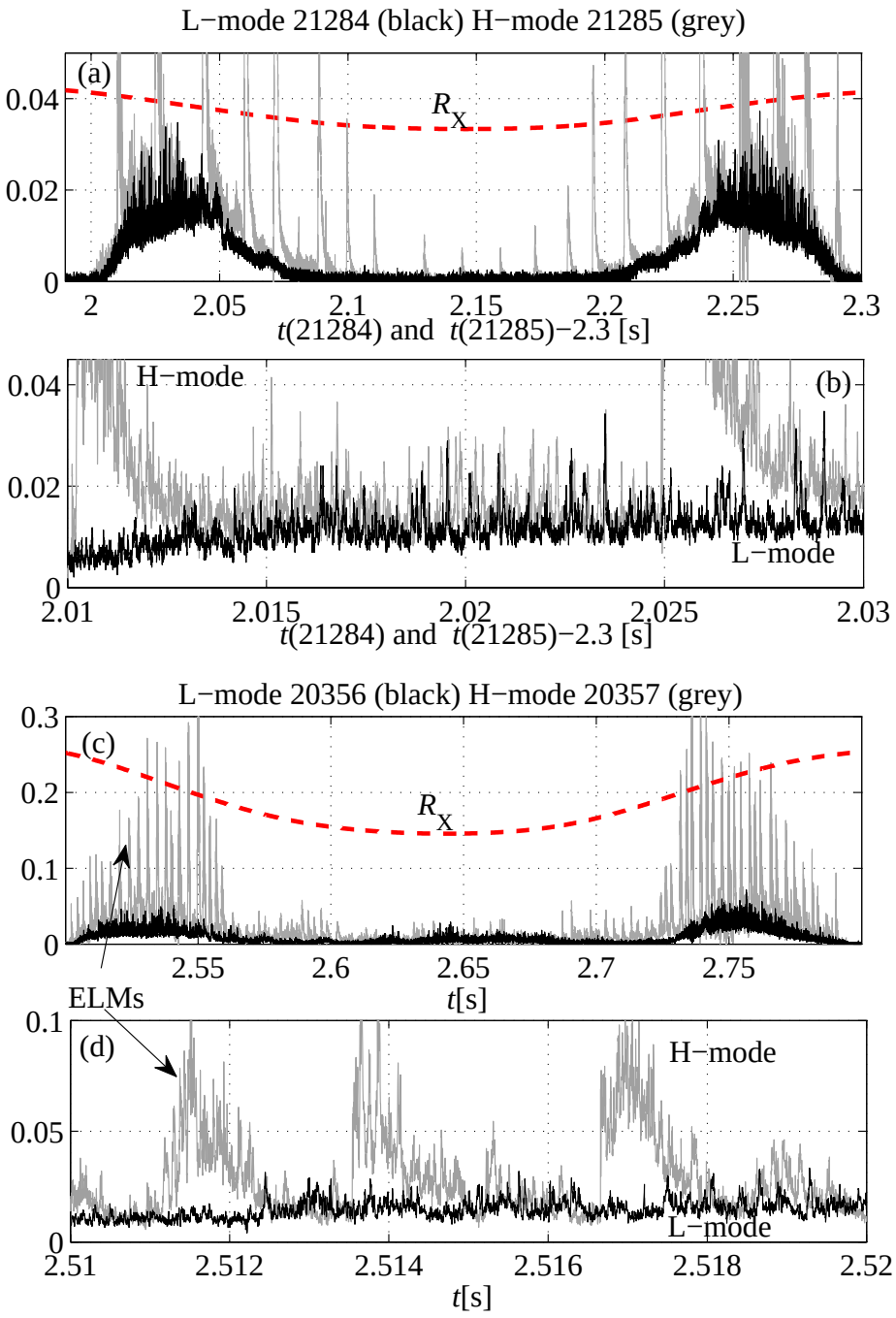

Figure 2. (a) illustrates the ion saturation current (I_{sat}) from the Langmuir probe for the two discharges 21284 and 21285; The dashed line illustrates the probe plunge as a function of time in arbitrary units. (b) is a zoom on (a) where the probe is on the low-field SOL. In (c), we represent the same plot as in (a) but for the shots 20356 and 20357. In (d) is shown a zoom on the I_{sat} signals of (c).

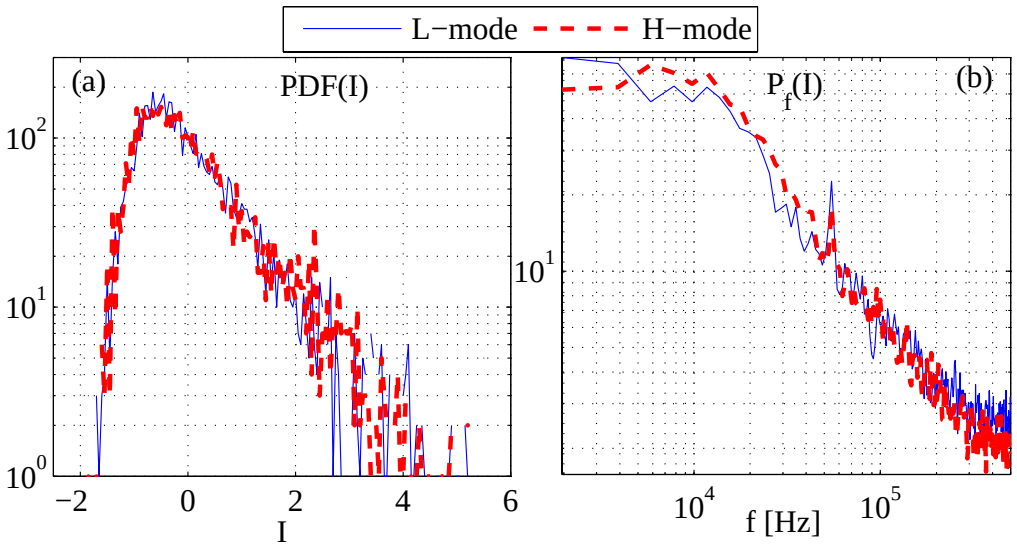

Figure 3. (a) and (b) represents respectively the PDF and the power spectrum (P_f) of I in L (solid) and H-mode (dashed) for shots 21284 and 21285.

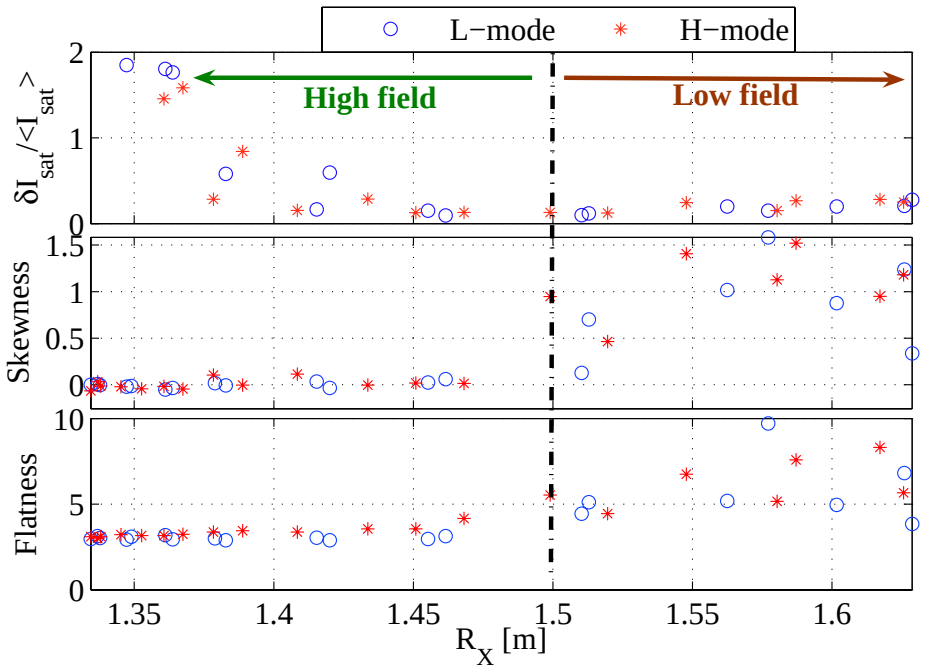

Figure 4. (a) the relative level of fluctuations ($\delta I_{sat}/\langle I_{sat}\rangle$) as a function of the probe position (R_X) in L-mode (o) and H-mode (*) from shots 21284 and 21285. δI_{sat} is the standard deviation of the fluctuations and the symbol $\langle\rangle$ represents time average. In (b) and (c) are plotted respectively the skewness ($\langle I^3\rangle/\langle I^2\rangle^{3/2}$) and the flatness ($\langle I^4\rangle/\langle I^2\rangle^2$) factors as a function of R_X.

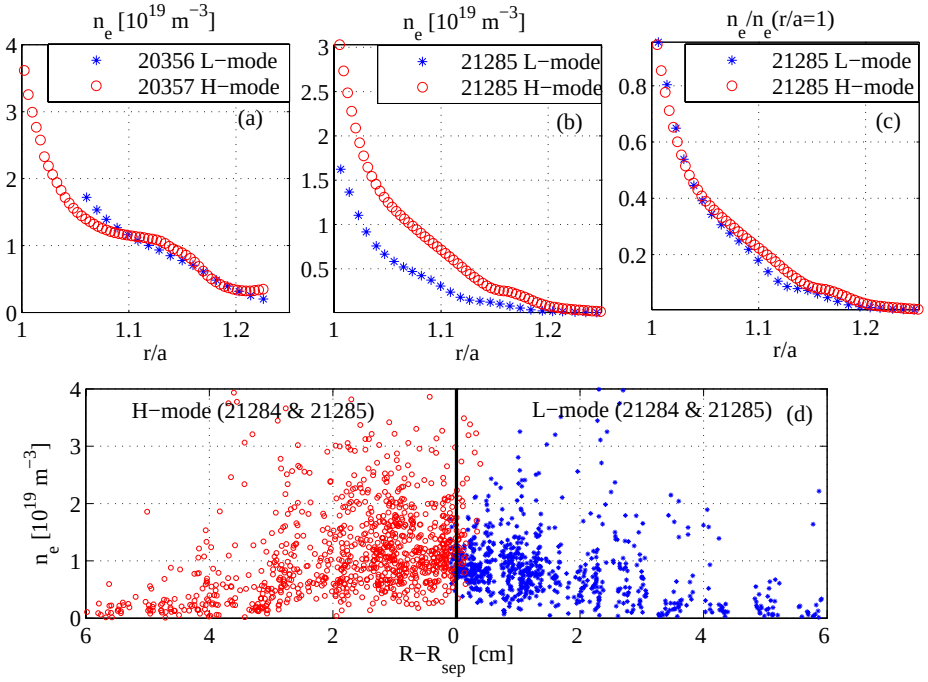

Figure 5. In (a) and (b) we plot the average density profile as a function of r/a using the lithium beam diagnostic. In (c) is shown the profiles of (b) normalized by the density at $r/a = 1$. In (d), we plot the profiles of the Thomson scattering of shots 21284 and 21285 when the plasma is in L-mode (right-hand side) and H-mode (left-hand side).